



CM-P00057069

THE HIGH-ENERGY BEHAVIOUR OF THE REAL PART OF THE  
ELASTIC SCATTERING AMPLITUDE

A. Białas <sup>\*)</sup> and E. Białas <sup>\*)</sup>

CERN - Geneva

A B S T R A C T

This paper discusses a relation between the high-energy behaviour of the real part of the elastic scattering amplitude and the high-energy behaviour of its imaginary part. Using the Phragmén-Lindelöf theorem we derive the formulae which express this relation. Under the assumption that the elastic amplitude becomes purely imaginary in the limit of infinite energy, these formulae suggest a simple five-parameter description of the high-energy behaviour of : i) the total cross-sections for the collisions  $A+\bar{B}$ , where  $\bar{B}$  is an antiparticle of  $B$ , and ii) the ratio  $X$  between the real and imaginary parts of the forward scattering amplitude for the corresponding elastic reactions. We proved that the existing data for nucleon-nucleon scattering can, in fact, be described in this way. We also checked that our results are consistent with the calculation based on the dispersion relations.

The asymptotic formulae also show that : a) from the fact that the total cross-sections are going down with energy, it follows that the real part of the forward scattering amplitude should be negative at high energies, and b) from the fact that the total  $p\bar{p}$  total cross-section changes with energy much more than the total  $pp$  cross-section, it follows that the absolute value of the ratio  $X$  should be smaller for  $p\bar{p}$  scattering than for the  $pp$  scattering.

We also considered the more general case when the ratio between the real and imaginary parts of the forward elastic amplitude tends to a non-vanishing limit at high energy. For nucleon-nucleon scattering the present day data suggest that the absolute value of the ratio  $X$  at infinite energy is smaller than 0.2.

---

\*) On leave from Jagellonian University, Cracow, Poland.

E R R A T A

THE HIGH-ENERGY BEHAVIOUR OF THE REAL PART OF THE  
ELASTIC SCATTERING AMPLITUDE

A. Białas and E. Białas

ABSTRACT : line 9 should read: "collisions  $A+B$  and  $A+\bar{B}$ ,  
where  $\bar{B} \dots$ "

page 1 : line 18 should read: "asymptotic behaviour of its  
imaginary part and by the asymptotic behaviour of the  
imaginary part for the crossed reaction <sup>3-6)</sup>."

page 16 : line 10 should read: "given by Eqs. (5.1) to (5.4)  
are given in Fig. 6."

page 21 : line 10 should read: "were calculated by Söding <sup>13)</sup>  
from dispersion relations."

10057/TH.504

## 1. Introduction

The purpose of this paper is a semi-phenomenological description of the high-energy behaviour of the elastic scattering amplitude. We would like to discuss here the relation between the high-energy behaviour of the real and imaginary parts of the elastic scattering amplitude in nucleon-nucleon scattering, taking into account the new experimental data:

- a) the measurements of the real part of the pp elastic amplitude at high energy<sup>1)</sup>;
- b) the recent measurements of the total cross-sections for the pp and  $\bar{p}p$  scattering in the region 6 - 25 GeV/c<sup>2</sup>).

The relation between the real and imaginary parts of the elastic amplitude follows from the analyticity properties as expressed, e.g., by the dispersion relations. The investigation of the dispersion relations in the high-energy region shows that, under some reasonable conditions which we will specify later on, the high-energy behaviour of the real part of the scattering amplitude is essentially determined by the asymptotic behaviour of the imaginary part for the crossed reaction<sup>3-6)</sup>. We rederive here these asymptotic relations<sup>7)</sup> using as main tool the Phragmén-Lindelöf theorem in a way proposed by Meiman<sup>8)</sup> and applied to similar problems by Logunov et al.<sup>9)</sup>, Van Hove<sup>10)</sup>, Khuri and Kinoshita<sup>6)</sup>. The argument we present applies to any pair of the crossed elastic reactions, provided one can neglect the spin dependence of the elastic scattering at high energy.

The relations we obtained, together with the optical theorem, suggest a simple parametrization of the high-energy behaviour of the following experimentally measurable quantities:

2.

- i) the ratios of the real to the imaginary parts of the forward elastic amplitude for two (direct and crossed) reactions;
- ii) the corresponding total cross-sections.

We discuss here in detail the case

$$\frac{\text{Re } T}{\text{Im } T} \xrightarrow{s \rightarrow \infty} 0 \quad (1.1)$$

where  $T$  is the forward scattering amplitude and  $s = (\text{c.m. energy})^2$ . In this case our description contains five free parameters. We applied it to the nucleon-nucleon scattering and found that it is possible to obtain a good fit to the experimental data<sup>1,2</sup>). The data on the total  $pp$  and  $p\bar{p}$  cross-sections and the ratio  $\text{Re } T/\text{Im } T$  for  $pp$  elastic forward scattering essentially fix four from our five parameters. This enables us to make a prediction on the high-energy behaviour of the ratio  $\text{Re } T/\text{Im } T$  for  $p\bar{p}$  forward elastic scattering.

From the asymptotic formulae and the assumption (1.1) one can also draw some qualitative conclusions which seem to be interesting because of their generality. One can see that there exists a correlation between the fact that all total cross-sections, as measured up to now, are going down with energy and the fact that the ratio  $\text{Re } T/\text{Im } T$  is negative at high energies. For the nucleon-nucleon scattering, from the fact that the total  $p\bar{p}$  cross-section varies with energy much more than the total  $pp$  cross-section, it follows that the absolute value of the ratio  $\text{Re } T/\text{Im } T$  should be smaller for  $p\bar{p}$  scattering than for  $pp$  scattering. This result shows clearly that one cannot consider separately the high-energy behaviour of the  $pp$  and  $p\bar{p}$  scattering. They are closely connected with each other.

Our argument can easily be generalized to include the case when  $\text{Re } T/\text{Im } T$  tends to a non-vanishing limit for infinite energy. This leads to an increase of the number of parameters by 1. We performed

the corresponding analysis for nucleon-nucleon scattering. The experimental data <sup>1,2)</sup> favour slightly the value  $|\text{Re } T/\text{Im } T|_{s=\infty}$  between 0 and 0.1. However, one cannot exclude the possibility of higher values (up to 0.2). It seems that the problem could be solved if precise data for small-angle  $p\bar{p}$  elastic scattering would be available.

## 2. The relation between the real and imaginary parts of the elastic scattering amplitude at high energies

We consider two crossed reactions

$$A + B \rightarrow A + B \quad (2.1)$$

and

$$A + \bar{B} \rightarrow A + \bar{B} \quad (2.2)$$

where the particles  $A$  and  $B$  are spinless and  $\bar{B}$  denotes the antiparticles of  $B$ . These two processes are described by the amplitudes  $T_1(s,t)$  and  $T_2(s,t)$  [ $t = -(\text{c.m. momentum transfer})^2$ ].

We will assume the following properties of the amplitudes  $T_1(s,t)$  and  $T_2(s,t)$  as functions of  $s$ , for fixed  $t$ :

- i)  $T_1(s,t)$  and  $T_2(s,t)$  are analytic and bounded by a polynomial in  $s$ , in the upper half  $s$  plane; apart from a finite interval they are continuous along the real axis.
- ii) For  $s \rightarrow \infty$  along the real axis, the amplitudes  $T_1(s,t)$  and  $T_2(s,t)$  can be expanded in the form:

$$T_1(s,t) \xrightarrow[t \text{ fixed}]{s \rightarrow +\infty} s \left[ ic(t) + \sum_{j=1}^N \frac{b_1^{(j)}(t)}{s^{\alpha_j(t)}} + \frac{d_1(t)}{s} \right] + \dots \quad (2.3)$$

$$T_2(s,t) \xrightarrow[t \text{ fixed}]{s \rightarrow +\infty} s \left[ ic^*(t) + \sum_{j=1}^N \frac{b_2^{(j)}(t)}{s^{\alpha_j(t)}} + \frac{d_2(t)}{s} \right] + \dots \quad (2.4)$$

The functions  $\alpha_j(t)$ ,  $j = 1 \dots N$ , are real.  $c(t)$ ,  $d_1(t)$ ,  $d_2(t)$  and  $b_1^{(j)}(t)$ ,  $b_2^{(j)}(t)$ ,  $j = 1 \dots N$ , can be complex.  $\alpha_j(t)$  satisfy the condition

$$0 < \alpha_1(t) < \alpha_2(t) \dots < \alpha_N(t) < 1. \quad (2.5)$$

The assumption i) is a standard assumption on the analytic properties of the scattering amplitude and we will not discuss it here. The assumption ii) needs, perhaps, some comments. The form of the first terms in the expansions (2.3) and (2.4) can be proved from the assumptions that (a) the amplitudes  $T_1$  and  $T_2$  do not oscillate as  $s \rightarrow \infty$  along the real axis, and (b) the total cross-sections and the differential elastic cross-sections tend to constant, non-vanishing values as  $s \rightarrow \infty$ <sup>10</sup>). The reality of  $\alpha_j(t)$  ensures that there are no oscillations in  $s$  also in the next terms of the expansion. The form of these terms is not the most general one which satisfies this condition. It was chosen because of its simplicity and because it is sufficient for the description of the present experimental data. More complicated terms as, for example,

$$\frac{l(t)}{s^{\mu(t)} (\ln s)^{\nu(t)} (\ln \ln s)^{\lambda(t)} \dots} \quad (2.6)$$

can, if needed, be introduced into the discussion. The condition (2.5) restricts our analysis to the terms in the cross-sections which do not decrease faster than  $1/s$ . As we are interested in the high-energy region, this restriction is (we believe) not very essential.

Let us now state the main result:

From the assumptions i) and ii) it follows

$$b_1^{(j)}(t) = b_2^{(j)*}(t) e^{-i\pi[1 - \alpha_j(t)]} \quad (2.7)$$

$$d_1(t) = d_2^*(t) - ic(t) \left[ 2(m_A^2 + m_B^2) - t \right] \quad (2.8)$$

where  $m_A$  and  $m_B$  denote the masses of particles A and B, respectively.

Written in full, the formulae (2.7) and (2.8) become

$$\operatorname{Re} b_1^{(j)}(t) = - \frac{\operatorname{Im} b_2^{(j)}(t) + \operatorname{Im} b_1^{(j)}(t) \cos \pi [1 - \alpha_j(t)]}{\sin \pi [1 - \alpha_j(t)]} \quad (2.7')$$

$$\operatorname{Re} b_2^{(j)}(t) = - \frac{\operatorname{Im} b_1^{(j)}(t) + \operatorname{Im} b_2^{(j)}(t) \cos \pi [1 - \alpha_j(t)]}{\sin \pi [1 - \alpha_j(t)]} \quad (2.7'')$$

$$\operatorname{Re} d_1(t) = \operatorname{Re} d_2(t) + \operatorname{Im} c(t) \left[ -t + 2(m_A^2 + m_B^2) \right] \quad (2.8')$$

$$\operatorname{Im} d_1(t) + \operatorname{Im} d_2(t) = \operatorname{Re} c(t) \left[ t - 2(m_A^2 + m_B^2) \right] . \quad (2.8'')$$

We see from the formulae (2.7') and (2.7'') that  $\operatorname{Re} b_1^{(j)}(t)$  and  $\operatorname{Re} b_2^{(j)}(t)$   $j = 1 \dots N$ , are fully determined by  $\operatorname{Im} b_1^{(j)}(t)$  and  $\operatorname{Im} b_2^{(j)}(t)$ . There is no such relation, however, for the functions  $d_1(t)$  and  $d_2(t)$ . This is a consequence of the fact that the analyticity properties i) imply for  $T_1$  and  $T_2$  dispersion relations with one subtraction.

We will now sketch the proof of the formulae (2.7) and (2.8). The proof we give here is a direct application of the method used in Refs. 8, 9 and 10.

Consider an auxiliary function

$$M_1(s, t) \equiv \frac{T_1(s, t) - i s c(t)}{(s + i)^{1 - \alpha_1(t)}} \quad (2.9)$$

From (2.3) we have

$$\lim_{\substack{s \rightarrow +\infty \\ t \text{ fixed}}} M_1(s, t) = b_1^{(1)}(t) . \quad (2.10)$$

6.

Let us now calculate  $\lim_{\substack{s \rightarrow -\infty \\ t \text{ fixed}}} M_1(s, t)$ . Taking into account crossing symmetry

$$T_1(s, t) = T_2^*(u, t) \quad (2.11)$$

we get

$$\begin{aligned} \lim_{\substack{s \rightarrow -\infty \\ t \text{ fixed}}} M(s, t) &= \lim_{\substack{u \rightarrow +\infty \\ t \text{ fixed}}} \frac{T_2^*(u, t) - ic(t)[-u - t + 2(m_A^2 + m_B^2)]}{[-u - t + 2(m_A^2 + m_B^2) + i]^{1 - \alpha_1(t)}} \\ &= \lim_{\substack{u \rightarrow +\infty \\ t \text{ fixed}}} \frac{T_2^*(u, t) + ic(t)u - ic(t)[2(m_A^2 + m_B^2) - t]}{[u + t - 2(m_A^2 + m_B^2) - i]^{1 - \alpha_1(t)} e^{i\pi[1 - \alpha_1(t)]}} \\ &= b_2^{(1)*}(t) e^{-i\pi[1 - \alpha_1(t)]} \end{aligned} \quad (2.12)$$

The function  $M_1(s, t)$  satisfies the analyticity properties listed in (i). Therefore we can apply to it the Phragmén-Lindelöf theorem which says

$$\lim_{\substack{s \rightarrow +\infty \\ t \text{ fixed}}} M_1(s, t) = \lim_{\substack{s \rightarrow -\infty \\ t \text{ fixed}}} M_1(s, t) \quad (2.13)$$

From the formulae (2.10), (2.12) and (2.13), we get

$$b_1^{(1)}(t) = b_2^{(1)*}(t) e^{-i\pi[1 - \alpha_1(t)]} \quad (2.14)$$



In a similar way, one can prove the equality (2.7) for the functions  $b_1^{(2)}(t)$  and  $b_2^{(2)}(t)$ , by considering the function

$$M_2(s,t) \equiv \frac{T_1(s,t) - isc(t) - b_1^{(1)}(t)(s+i)^{1-\alpha_1(t)}}{(s+i)^{1-\alpha_2(t)}}, \quad (2.15)$$

taking into account the equality (2.14) and applying the Phragmén-Lindelöf theorem. The generalization for all  $j = 3, 4, \dots, N$  is obvious.

To prove the formula (2.8) let us consider the function

$$N(s,t) \equiv T_1(s,t) - isc(t) - \sum_{j=1}^N b_1^{(j)}(t)(s+i)^{1-\alpha_j(t)}. \quad (2.16)$$

From (2.13) and (2.16) we have

$$\lim_{\substack{s \rightarrow \infty \\ t \text{ fixed}}} N(s,t) = d_1(t). \quad (2.17)$$

One should calculate now  $\lim_{\substack{s \rightarrow -\infty \\ t \text{ fixed}}} N(s,t)$ . Taking into account (2.7) and (2.11) we get

$$\begin{aligned} \lim_{\substack{s \rightarrow -\infty \\ t \text{ fixed}}} N(s,t) &= \lim_{\substack{u \rightarrow +\infty \\ t \text{ fixed}}} \left\{ T_2^*(u,t) - ic(t) \left[ -u - t + 2 \left( m_A^2 + m_B^2 \right) \right] \right. \\ &\quad \left. - \sum_{j=1}^N b_1^{(j)}(t) \left[ -u - t + 2 \left( m_A^2 + m_B^2 \right) + i \right]^{1-\alpha_j(t)} \right\} \\ &= \lim_{\substack{u \rightarrow +\infty \\ t \text{ fixed}}} \left\{ T_2^*(u,t) + ic(t)u - \sum_{j=1}^N b_1^{(j)} e^{i\pi[1-\alpha_j(t)]} \right. \\ &\quad \left. \times \left[ u + t - 2 \left( m_A^2 + m_B^2 \right) - i \right]^{1-\alpha_j(t)} - ic(t) \left[ 2 \left( m_A^2 + m_B^2 \right) - t \right] \right\} = \end{aligned}$$

8.

$$\begin{aligned}
 &= \lim_{\substack{u \rightarrow +\infty \\ t \text{ fixed}}} \left\{ T_2^*(u, t) + ic(t)u - \sum_{j=1}^N b_2^{(j)*}(t) \right. \\
 &\quad \left. \left[ u + t - 2 \left( m_A^2 + m_B^2 \right) - i \right]^{1 - \alpha_j(t)} \right. \\
 &\quad \left. - ic(t) \left[ 2 \left( m_A^2 + m_B^2 \right) - t \right] \right\} \\
 &= d_2^*(t) - ic(t) \left[ 2 \left( m_A^2 + m_B^2 \right) - t \right] .
 \end{aligned} \tag{2.18}$$

From (2.17), (2.18) and the Phragmén-Lindelöf theorem we have (2.8) Q.E.D.

### 3. Forward elastic scattering

The case of the forward scattering is especially interesting because for  $t = 0$  one can calculate the imaginary part of the elastic amplitude in terms of the total cross-section from the optical theorem:

$$\text{Im } T(s, 0) = \frac{k_{\text{c.m.}} \sqrt{s}}{8\pi^2} \sigma^T(s) \tag{3.1}$$

where  $\sigma^T$  is the total cross-section and  $k_{\text{c.m.}}$  is the c.m. momentum of the colliding particles.

We will assume that, in the high-energy region, the total cross-sections for the reactions (2.1) and (2.2) are represented with a good accuracy by the formulae:

$$\sigma_1^T = \sigma_\infty + \frac{A_1}{s} \quad (3.2)$$

$$\sigma_2^T = \sigma_\infty + \frac{A_2}{s} \quad (3.3)$$

where  $\sigma_\infty$ ,  $\alpha$ ,  $A_1$  and  $A_2$  are constants. The formulae (3.2) and (3.3) are the simplest ones which agree with the expansions (2.3), (2.4). They seem to approximate rather well the experimental values of total cross-sections for all reactions measured up to now, in the energy range  $\geq 5$  GeV/c.

The values of the constants  $\sigma_\infty$ ,  $\alpha$ ,  $A_1$  and  $A_2$  one can find from the fit to the experimental values of the cross-sections. Once we know them we can calculate from (3.1) the imaginary part of the amplitudes (2.3), (2.4) for  $t=0$ . The formulae (2.7) and (2.8) give us then the asymptotic behaviour of the real part of the forward amplitude in terms of two parameters  $B \equiv 16\pi^2 \frac{\text{Re} \alpha(\sigma_1^T(\mu_A^2 + \mu_B^2) \sin c_0)}{\text{Im} d_2(0)}$  and  $D = 16\pi^2 \text{Im} c(0)$ . After some simple algebra we obtain

$$X_1(s) \equiv \frac{\text{Re } T_1(s,0)}{\text{Im } T_1(s,0)} = - \frac{A_2 + A_1 \cos \pi(1-\alpha)}{s \sigma_1^T(s) \sin \pi(1-\alpha)} + \frac{[B - 2(\frac{m_A^2}{A} + \frac{m_B^2}{B})D]}{s \sigma_1^T} - \frac{D}{\sigma_1^T} \quad (3.4)$$

$$X_2(s) \equiv \frac{\text{Re } T_2(s,0)}{\text{Im } T_2(s,0)} = - \frac{A_1 + A_2 \cos \pi(1-\alpha)}{s \sigma_2^T(s) \sin \pi(1-\alpha)} + \frac{B}{s \sigma_2^T} + \frac{D}{\sigma_2^T} \quad (3.5)$$

or

$$X_1(s) = - \frac{(\sigma_2^T - \sigma_\infty) + (\sigma_1^T - \sigma_\infty) \cos \pi(1-\alpha)}{\sigma_1^T \sin \pi(1-\alpha)} + \frac{[B - 2(\frac{m_A^2}{A} + \frac{m_B^2}{B})D]}{s \sigma_1^T} - \frac{D}{\sigma_1^T} \quad (3.6)$$

$$X_2(s) = - \frac{(\sigma_1^T - \sigma_\infty) + (\sigma_2^T - \sigma_\infty) \cos \pi(1-\alpha)}{\sigma_1^T \sin \pi(1-\alpha)} + \frac{B}{s \sigma_2^T} + \frac{D}{\sigma_2^T} \quad (3.7)$$

The formulae (3.4) and (3.5) or (3.6) and (3.7) can be applied to any pair of crossed elastic reactions, provided we neglect the spin dependence of the amplitudes. Together with the formulae (3.2), (3.3) they represent a parameterization of the high-energy elastic and total cross-sections which contains six parameters. If one assumes that at high energy the elastic amplitude becomes purely imaginary, i.e.,

$$\left\{ \lim_{s \rightarrow \infty} X_1 = \lim_{s \rightarrow \infty} X_2 = 0 \right\} \longleftrightarrow \left\{ D = 0 \right\} \quad (3.8)$$

then one is left with five parameters.

Before we come in the next Section to the quantitative study of the relations (3.4) - (3.7) we would like to discuss some general conclusions which can be drawn from them on the basis of the existing experimental data. We will assume here the condition (3.8). We will also neglect the term  $B/s^\pi$  which at high energy represents (we believe) only a small correction and does not disturb the general picture.

The total cross-sections for all reactions measured up to now decrease with increasing energy of the incident particles. This means that the constants  $A_1$  and  $A_2$  are positive. It follows from this that if the values of  $\alpha$  are restricted to the region<sup>11)</sup>

$$\cos \pi(1-\alpha) > -\min \left( \frac{A_1}{A_2}, \frac{A_2}{A_1} \right) \quad (3.9)$$

then

$$X_1 < 0 \quad X_2 < 0 \quad (3.10)$$

i.e., the real part of the forward scattering amplitude is negative at high energies. Both the conditions (3.9) and (3.10) are in agreement with the experimental data for nucleon-nucleon and pion-nucleon collisions.

Consider now the special case of the nucleon-nucleon scattering. It is well-known that  $\sigma_{pp}^T$  is almost constant in the region of energy higher than 10 GeV, whereas  $\sigma_{pp}^{\bar{T}}$  changes rather appreciably in this region. This means that

$$A_{pp} \ll A_{pp}^- \quad . \quad (3.11)$$

The inequality (3.11) and the relations (3.4), (3.5) (with  $B = D = 0$ ) imply

$$\frac{X_{pp}^-}{X_{pp}} \approx \frac{\sigma_{pp}^T}{\sigma_{pp}^{\bar{T}}} \cos \pi(1-\alpha) < 1 \quad . \quad (3.12)$$

This result may be surprising at first sight<sup>1,2)</sup>. It shows that one cannot consider the asymptotic behaviour of the pp scattering separately from the  $pp^-$  scattering, and that the pp scattering is not "more asymptotic" in the region 10 - 25 GeV than the  $pp^-$  scattering.

#### 4. Nucleon-nucleon scattering: a study of the experimental data

In this Section we will consider in some detail the nucleon-nucleon scattering, taking into account the recent experimental data<sup>1,2)</sup>. We parameterize the experimental values of the total pp and  $pp^-$  cross-sections<sup>2)</sup> in the region 6 - 26 GeV/c in a way described in Section 3:

$$\sigma_{pp}^T = \sigma_{\infty}^{NN} + \frac{A_{pp}}{s^{\alpha_{NN}}} \quad (4.1)$$

$$\sigma_{pp}^{\bar{T}} = \sigma_{\infty}^{NN} + \frac{A_{pp}^-}{s^{\alpha_{NN}}} \quad . \quad (4.2)$$

Unfortunately, the existing measurements of the total pp and  $p\bar{p}$  cross-sections at high energy are not sufficiently accurate to determine uniquely the parameters  $\alpha_{NN}$ ,  $\sigma_{\infty}^{NN}$ ,  $A_{pp}$  and  $A_{p\bar{p}}$  which appear in the expansions (4.1) and (4.2). The situation is as follows: for a given value of  $\alpha_{NN}$  the parameters  $\sigma_{\infty}^{NN}$ ,  $A_{pp}$  and  $A_{p\bar{p}}$  can be determined with a reasonable accuracy (generally the error is smaller than 10%). The values of  $\alpha_{NN}$ , however, cannot be obtained from the fit - there exist fits corresponding to the probability higher than 5% (two standard deviations) for all  $\alpha_{NN}$  in the range

$$0.4 \leq \alpha_{NN} \leq 0.9 \quad . \quad (4.3)$$

Therefore we will discuss the further results in terms of  $\alpha_{NN}$ , which we will treat as a free parameter, changing in the range (4.3). The results of the analysis of the total cross-sections are summarized in Table 1.

TABLE 1

$\alpha_{NN}$	$\sigma_{\infty}^{NN}$ (mb)	$A_{pp}$ [mb (GeV) $^{2\alpha_{NN}}$ ]	$A_{p\bar{p}}$ [mb (GeV) $^{2\alpha_{NN}}$ ]
0.4	35.5	14.2	71
0.5	36.2	15.9	93
0.6	36.7	18.5	123
0.7	37.1	21.4	161
0.8	37.4	25.6	213
0.9	37.6	31.4	281

In terms of the parameters  $\alpha_{NN}$ ,  $\sigma_{\infty}^{NN}$ ,  $A_{pp}$  and  $A_{pp}^-$ , the ratios of the real to the imaginary part of the forward pp and  $\bar{p}\bar{p}$  elastic amplitude become

$$X_{pp} = - \frac{A_{pp}^- + A_{pp} \cos \pi(1 - \alpha_{NN})}{s^{\alpha_{NN}} \sigma_{pp}^T \sin \pi(1 - \alpha_{NN})} + \frac{Y \sigma_{\infty}^{NN}}{s \sigma_{pp}^T} - \frac{X_{\infty} \sigma_{\infty}^{NN}}{\sigma_{pp}^T} \quad (4.4)$$

$$X_{pp}^- = - \frac{A_{pp} + A_{pp}^- \cos \pi(1 - \alpha_{NN})}{s^{\alpha_{NN}} \sigma_{pp}^T \sin \pi(1 - \alpha_{NN})} + \frac{Y \sigma_{\infty}^{NN}}{s \sigma_{pp}^T} + \frac{X_{\infty} \sigma_{\infty}^{NN}}{\sigma_{pp}^T} \quad (4.5)$$

where  $X_{\infty}$  is the value of  $X_{pp}^-$  at  $s \rightarrow \infty$ .  $Y$  is a free parameter which represents the influence of the low-energy scattering on the high-energy behaviour of  $X_{pp}$  and  $X_{pp}^-$ . One can easily see that

$$- \lim_{s \rightarrow \infty} X_{pp}^- = \lim_{s \rightarrow \infty} X_{pp} = -X_{\infty} \quad (4.6)$$

For a few fixed values of  $\alpha_{NN}$  and  $X_{\infty}$  we tried to fit the formula (4.4) to the recent experimental data obtained by Belletini et al.<sup>1)</sup> The results are shown in Table 2. The table contains the values of  $Y$  obtained from the best fit to the three points given by Belletini et al. In parenthesis we also give the value of  $\chi^2$ . The values of  $Y$  as given in Table 2 should be understood to have an error  $\pm 0.9$ . The corresponding uncertainty of  $X_{pp}$  is  $\pm 0.04$  at 10 GeV/c and  $\pm 0.02$  at 20 GeV/c. For  $X_{pp}^-$  the uncertainty due to the error of  $Y$  is slightly smaller.

TABLE 2

$\alpha_{NN}$ \backslash $X_{\infty}$	0	0.1	0.2
0.4	2.6 (0.6)	5.6 (3.8)	8.6 (10.9)
0.5	2.2 (0.3)	5.3 (1.8)	8.3 (6.9)
0.6	2.7 (0.7)	5.7 (0.7)	8.7 (4.5)
0.7	4.1 (1.5)	7.2 (0.3)	10.2 (2.9)
0.8	8.8 (2.4)	11.8 (0.2)	14.9 (2.1)
0.9	26.0 (2.8)	29.0 (0.3)	32.1 (1.7)

From Table 2, one can see that

(a) if  $X_{\infty} = 0$  (i.e., the diffraction picture holds for high-energy nucleon-nucleon scattering) the small values of  $\alpha_{NN}$  ( $\alpha_{NN} \sim 0.5$ ) give a better fit to the data. It is impossible, however, to reject any of the values of  $\alpha_{NN}$ ;

(b) the values  $X_{\infty} > 0.2$  seem to be rather improbable. The data favour slightly the values between 0 and 0.1;

(c) an improvement of the experimental accuracy by 50% would provide a lot of information. It would probably solve the question of whether  $X_{\infty} = 0$  for nucleon-nucleon scattering.

Figures 1 and 2 show the plots of the functions  $X_{pp}$  and  $X_{pp}^-$ , respectively, for  $X_{\infty} = 0$ . The different curves correspond to the different values of  $\alpha_{NN}$ . Other parameters are chosen according to the Tables 1 and 2. We also plot the experimental points given by Belletini et al.<sup>1)</sup>.



One can see from Fig. 1 that the measurements of  $X_{pp}$  for the lab. momentum  $\sim 7$  GeV/c and  $\sim 35$  GeV/c would provide a large amount of information useful for further more detailed investigation.

To see how the situation changes if  $X_\infty \neq 0$ , we plot in Fig. 3 the function  $X_{pp}$  for  $X_\infty = 0.1$  and  $0.2$ . The corresponding values of  $\alpha_{NN}$  are  $0.8$  and  $0.9$ . These two curves represent the best fit to the data of Belletini et al.<sup>1)</sup> which one can get with  $X_\infty = 0.1$  and  $0.2$ , respectively. Once more we see that the critical regions from which one can expect most information are around  $7$  and  $35$  GeV/c. It would be very useful to have precise measurements of  $X_{pp}$  at these points.

Figures 4 and 5 give the plots of the function  $X_{pp}^-$  for  $X_\infty = 0.1$  and  $0.2$ , respectively. We see that the values of  $X_{pp}^-$  are very sensitive to  $X_\infty$  and  $\alpha_{NN}$ . Therefore the measurement of  $X_{pp}^-$  at high energy will provide an essential tool in further analysis of the situation.

##### 5. The comparison with the dispersion relations

To get an idea as to whether our approach is consistent with the dispersion relations, we compared our results with those obtained by Söding<sup>13)</sup>. Söding used the values

$$\alpha = 0.72 \quad \sigma_\infty = 39 \text{ mb} \quad . \quad (5.1)$$

He does not quote, however, the values of  $A_{pp}$  and  $A_{pp}^-$ . Therefore we determined the values of  $A_{pp}$  and  $A_{pp}^-$  by a fit to the experimental data used in our paper<sup>2)</sup> with  $\alpha$  and  $\sigma_\infty$  given by (5.1). We found

$$A_{pp} = 4 \text{ mb}(\text{GeV})^{1.44} \quad A_{pp}^- = 150 \text{ mb}(\text{GeV})^{1.44} \quad (5.2)$$

Taking into account the values (5.1), (5.2) and the condition

$$X_{\infty} = 0 \quad (5.3)$$

which was used by Söding, we found the value of  $Y$  for which, at 10 GeV/c, the function  $X_{pp}$  is equal to 0.3, i.e., the value given by Söding. This is the case for

$$Y = 5.6 \text{ (GeV)}^2 \quad (5.4)$$

The formulae (5.1) to (5.4) fix all our parameters in a way which is (we believe) as close as possible to that used by Söding<sup>14</sup>).

The plots of the functions  $X_{pp}$  and  $X_{-pp}$  for the parameters given by Eqs. (5.1) to (5.4) are given in Fig. 5. In the same Figure we also plotted the corresponding curves from Söding's paper. One can see that our calculations reproduce the dispersion relation calculations with a very good accuracy. This shows that the calculations of the high-energy behaviour of the real part of the forward elastic amplitude by means of the dispersion relations are essentially equivalent to the evaluation of a single parameter  $Y$ . This parameter depends on the low-energy behaviour of the cross-sections and also (in the nucleon-nucleon case) on the shape of the imaginary part of the amplitude in the unphysical region. Its exact evaluation from the dispersion relations is impossible in the case of nucleon-nucleon scattering, because of the existence of the large unphysical region. Therefore our approach, in which we find the value of  $Y$  from the high-energy data, seems to be useful for the phenomenological study of the problem. At the moment it contains less free parameters than the calculations based on the dispersion relations.

## 6. Conclusions

Our conclusions can be summarized in the following points.

(i) We developed a method of parameterization of the high-energy total cross-sections and forward elastic amplitudes based on the asymptotic formulae which follow from the analyticity of the scattering amplitudes. This method is much simpler than the calculations by means of the dispersion relations: the formulae are very compact and do not contain any complicated integrals.

(ii) We found that our method can reproduce the results of the calculations of the real part of the forward elastic amplitude from dispersion relations (in the energy region  $> 5$  GeV) with a good accuracy. This provides, (in our opinion), a good check for the validity of our approach.

(iii) The behaviour of the nucleon-nucleon forward elastic scattering for laboratory momentum  $> 6$  GeV/c can be described by the asymptotic formulae derived from the analyticity properties of the scattering amplitudes. This suggests that the region of energy  $> 6$  GeV is really an "asymptotic region".

(iv) The nucleon-nucleon data are consistent with the assumption that the forward elastic amplitude becomes purely imaginary at high energies:

$$\frac{\text{Re } T}{\text{Im } T} \xrightarrow{s \rightarrow \infty} 0 \quad (6.1)$$

The other possibility cannot be excluded, but our analysis suggests that for the pp elastic scattering, we have an inequality

$$\left| \frac{\text{Re } T}{\text{Im } T} \right|_{s=\infty} < 0.2 \quad (6.2)$$

(v) Our asymptotic formulae, together with the assumption (5.1), show that a) there exists a relation between the fact that all total cross-sections are going down with the energy in the high-energy region and the fact that the real part of the forward elastic amplitude is negative, and b) the real part of the forward elastic amplitude at high energy should be bigger for  $pp$  scattering than for the  $p\bar{p}$  scattering. The relation (b) follows from the fact that, in the energy region considered, the total  $p\bar{p}$  total cross-section changes much more with the energy than the total  $pp$  cross-section.

(vi) Precise measurements of the real part of the  $p\bar{p}$  forward scattering amplitude will probably be of great help in proving or disproving the condition (6.1) for nucleon-nucleon scattering.

(vii) The most interesting energy regions for the measurements of the real part of the  $pp$  forward elastic amplitude seem to be 7 and 35 GeV/c.

#### Acknowledgements

The authors would like to thank Professor L. Van Hove for the very helpful discussions and encouragement, and for the hospitality extended to them at CERN. They are very grateful to Professors G. Cocconi and A.N. Diddens for the communication of unpublished results. They have also greatly profited from discussions with Drs. O Czyzewski, K. Dietz and L. Michejda.

REFERENCES AND FOOTNOTES

1. For pp scattering we used the data from the last CERN experiment:  
G. Belletini, G. Cocconi, A.N. Diddens, E. Lillethun, J. Pahl,  
J.P. Scanlon, J. Walters, A.M. Wetherell, and P. Zanella (private  
communication - to be published in Phys. Letters).
2. We used the data from the Brookhaven and CERN experiments:  
for pp scattering  
(a) see Ref. 1,  
(b) W. Galbraith, E.W. Jenkins, T.F. Kycia, B.A. Leontic,  
R.H. Phillips, A.L. Read and R. Rubinstein, Report at the  
International Conference on High-Energy Physics, Dubna,  
USSR (August 1964);  
for  $\bar{p}p$  scattering  
S.J. Lindenbaum, W.A. Love, J.A. Niederer, S. Ozaki,  
J.J. Russel, and L.C.L. Yuan, Phys.Rev. Letters 7, 185 (1962).
3. H. Lehmann, Nuclear Phys. 29, 300 (1964).
4. V.S. Barashenkov, Fortschritte der Physik 10, 205 (1962).
5. J. Hamilton and W.S. Woolcock, Rev.Mod.Phys. 35, 737 (1963).
6. N.N. Khuri and T. Kinoshita "The Real Part of the Scattering Amplitude and the Behaviour of the Total Cross-Section at High Energies", preprint.
7. These relations have been discussed recently in the case of the pion-proton scattering by P.G.O. Freund, Phys.Letters 5, 341 (1963), by G. Höhler, G. Ebel and J. Giesecke, Zeitschrift für Physik, 180, 430 (1964), and by P. Olesen, Phys.Letters 13, 175 (1964).

8. N.N. Meiman, Zh.Experim. i Teor.Fiz. 43, 2277 (1962). English translation: Soviet Physics JETP 16, 1609 (1963).
9. A.A. Lugonov, N. Van Hieu, I.T. Todorov and O.A. Khrustalev, Phys.Letters 7, 69 (1963).
10. L. Van Hove, Rev.Mod.Phys. 36, 655 (1964) and also "Theoretical Problems in Strong Interactions at High Energies", CERN lecture notes, part III (1964).
11. The condition (3.8) is always satisfied if  $0.5 < \alpha < 1$ .
12. The same result was obtained by Söding, see Ref. 13.
13. P. Söding, Phys.Letters 8, 285 (1964).
14. Söding used, in fact, two different values of  $\alpha$  for pp and  $p\bar{p}$  scattering ( $\alpha_{pp} > \alpha_{p\bar{p}}$ ). Therefore one can argue that we should take  $A_{pp} = 0$ . This, however, makes no difference to the results.

Figure captions

- Fig. 1. The ratio  $X_{pp}$  for  $X_{\infty} = 0$  and different values of  $\alpha_{NN}$ . The experimental points are taken from Ref. 1.
- Fig. 2. The ratio  $X_{pp}$  for  $X_{\infty} = 0$  and different values of  $\alpha_{NN}$ .
- Fig. 3. The ratio  $X_{pp}$  for  $X_{\infty} = 0.1$  and  $0.2$ . The experimental points are taken from Ref. 1.
- Fig. 4. The ratio  $X_{pp}$  for  $X_{\infty} = 0.1$  and different values of  $\alpha_{NN}$ .
- Fig. 5. The ratio  $X_{pp}$  for  $X_{\infty} = 0.2$  and different values of  $\alpha_{NN}$ .
- Fig. 6. The comparison with dispersion relations. The dotted curves were calculated by Söding<sup>11)</sup> from dispersion relations. The continuous curves result from our calculations.

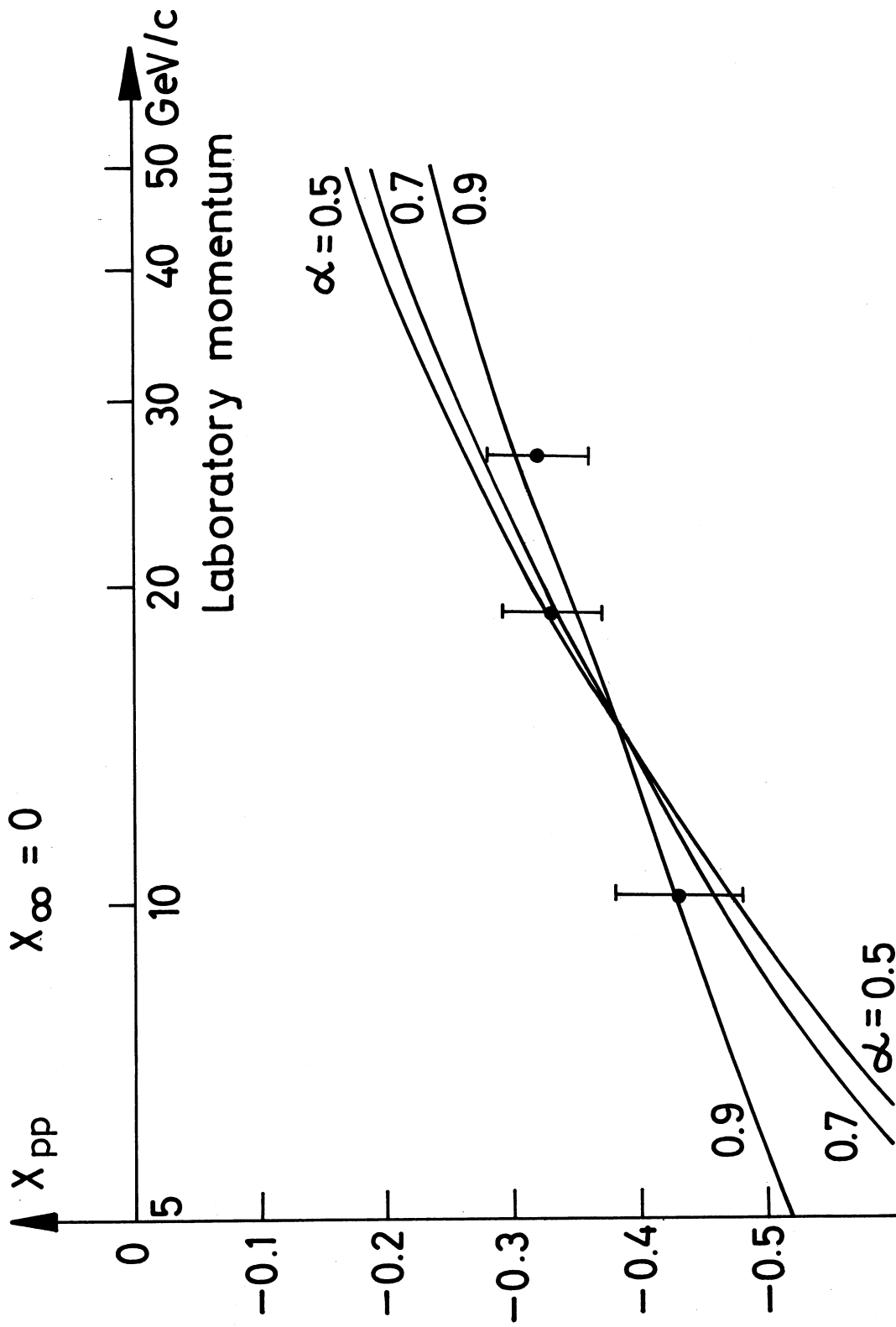


FIG. 1



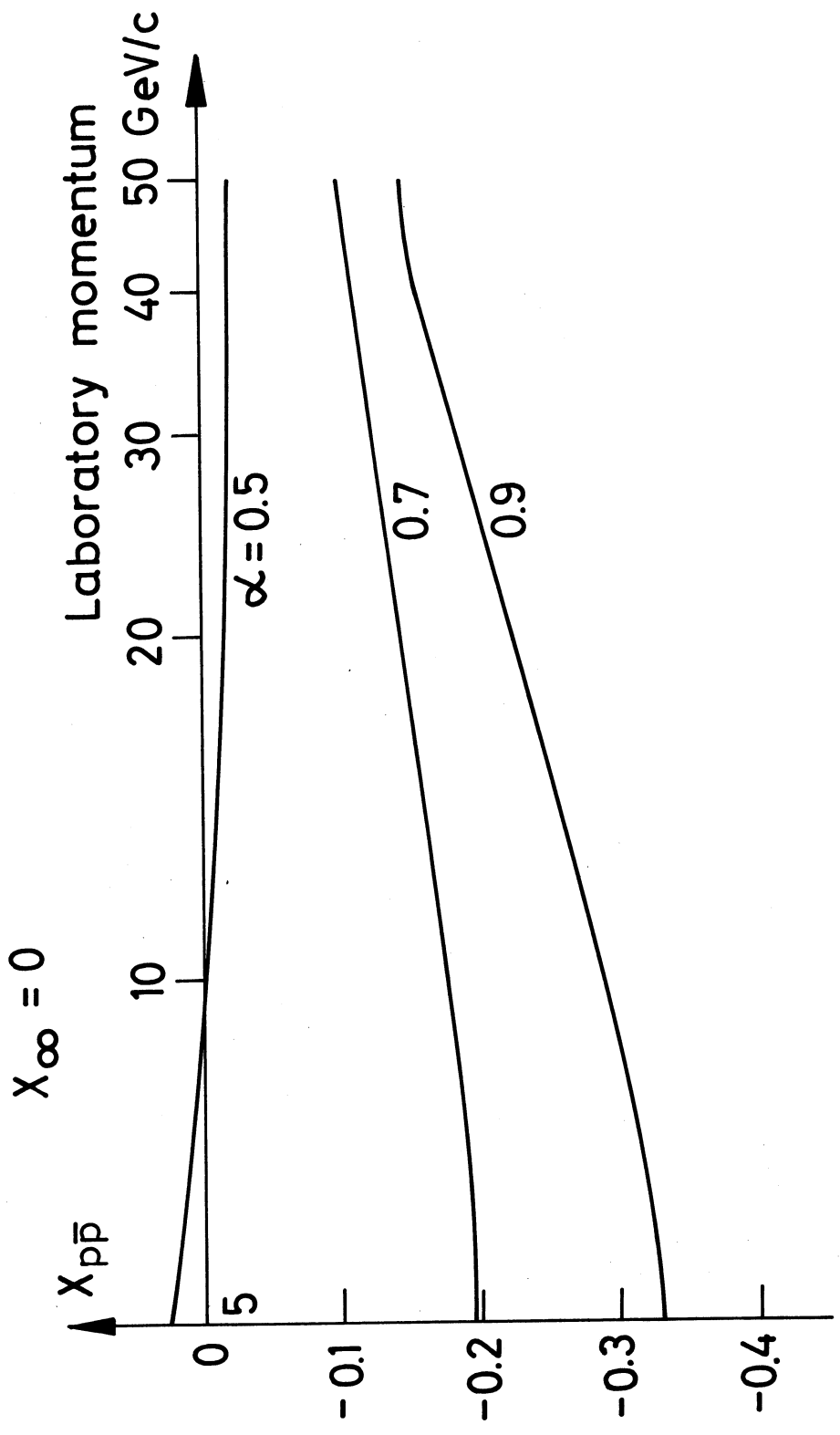


FIG. 2

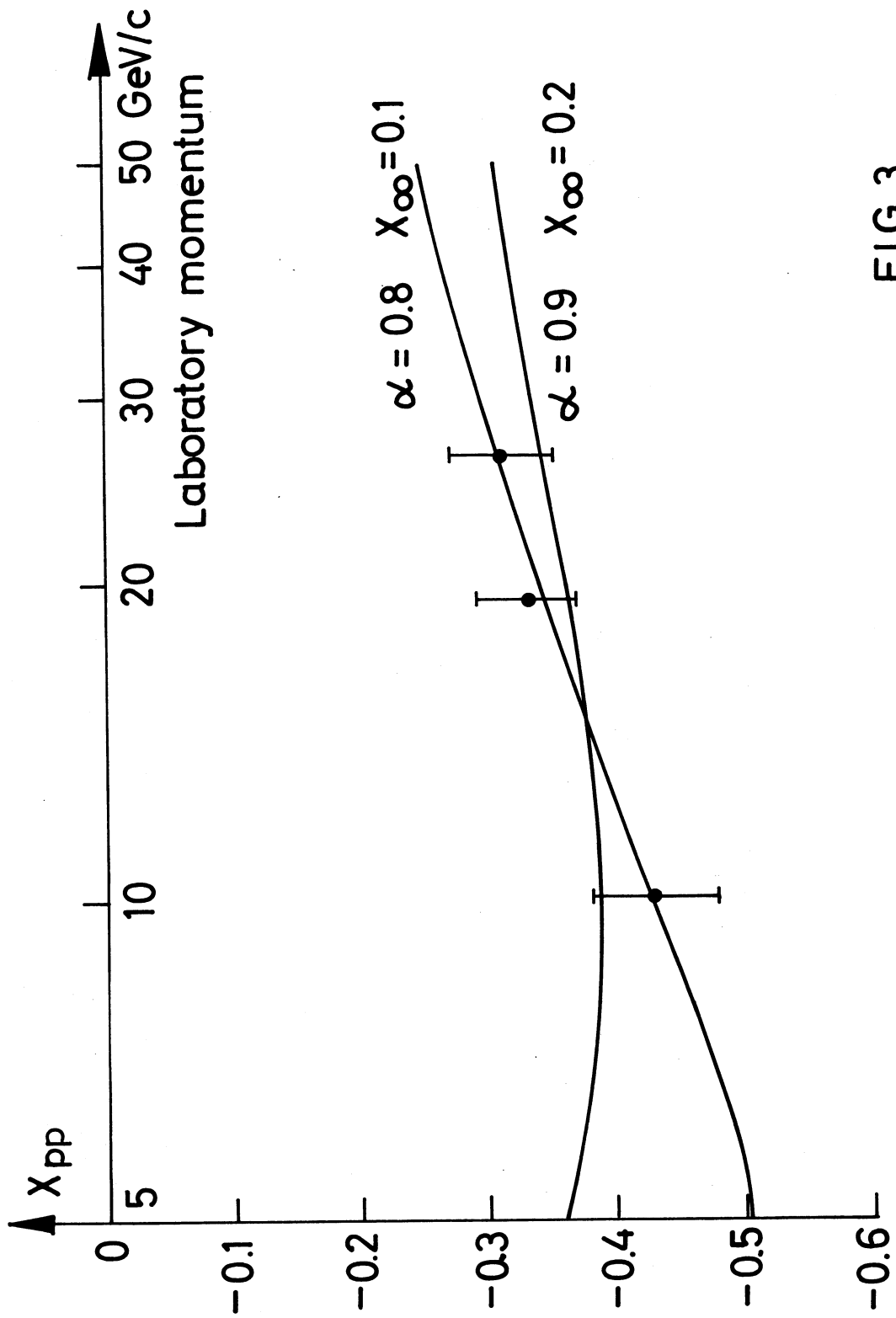


FIG. 3

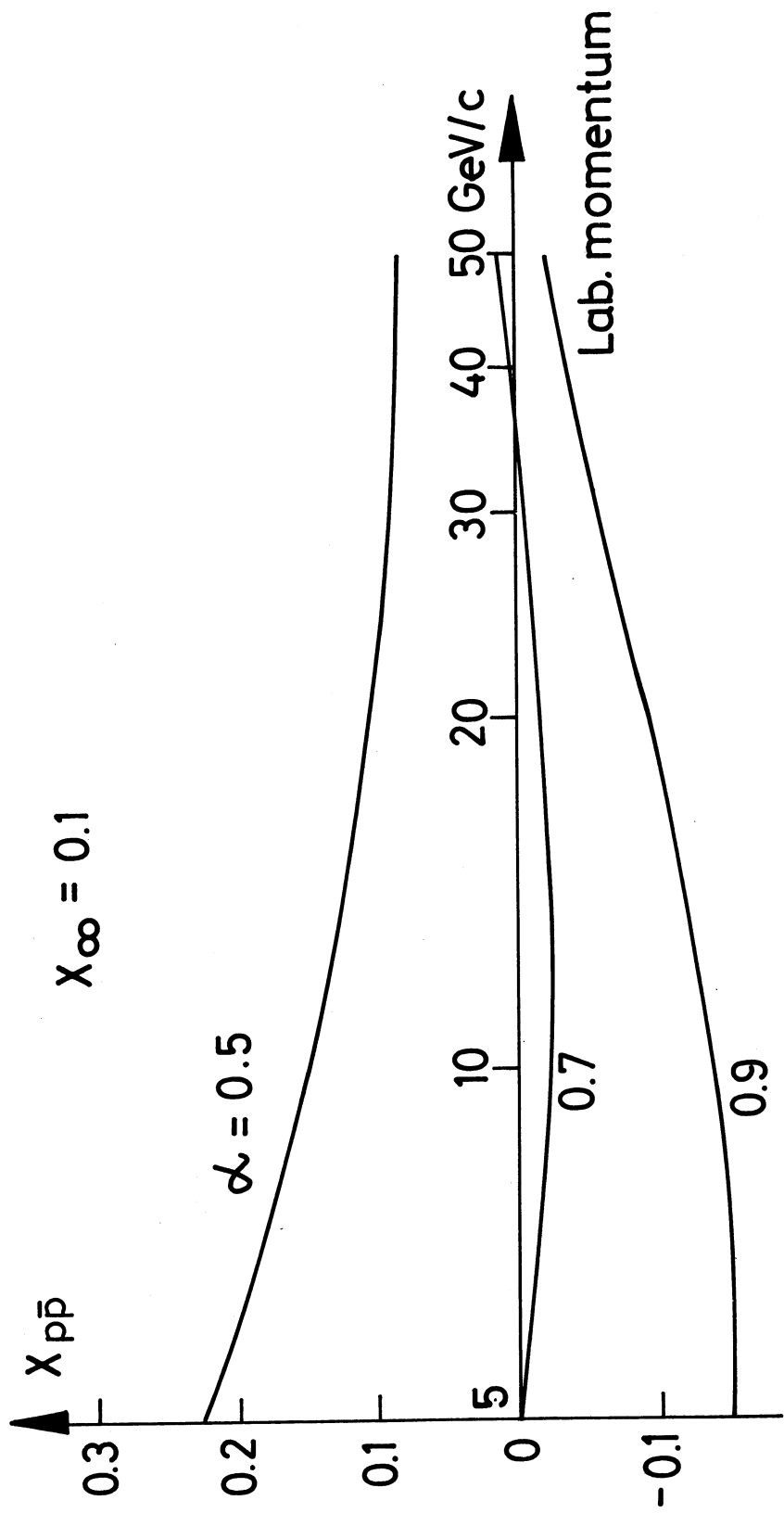


FIG. 4

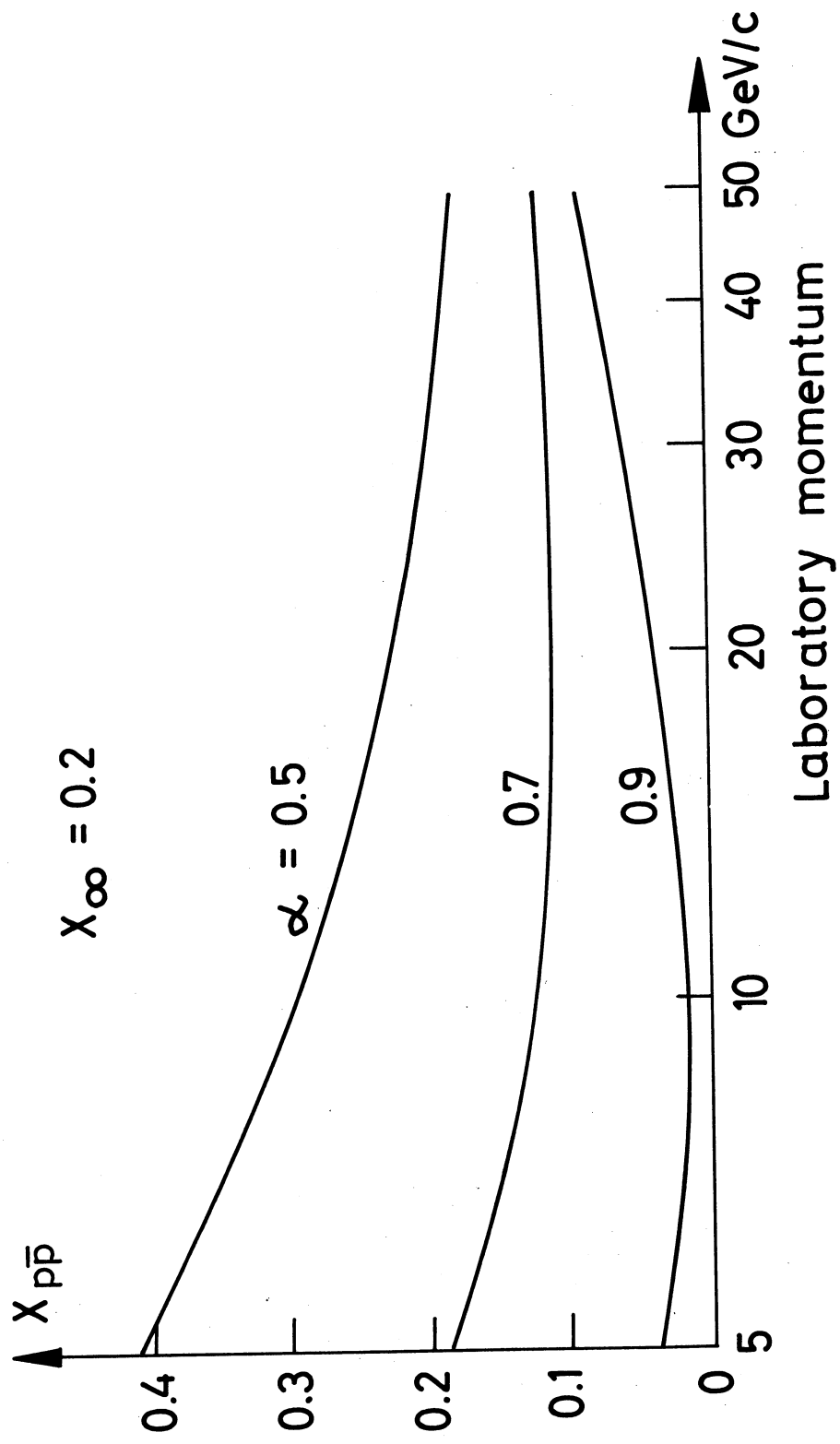


FIG.5

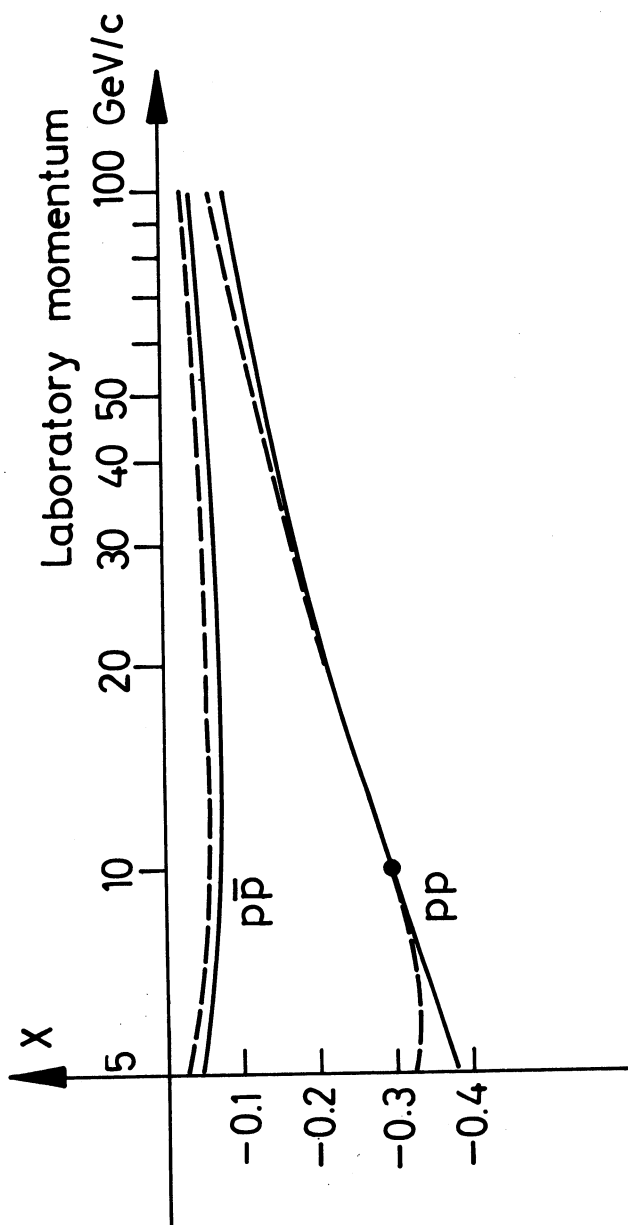


FIG. 6